Electric Field Enhanced Ammoxidation of Aldehydes Using Supported Fe Clusters Under Ambient Oxygen Pressure

Chao Wang, Jialu Li, Tianyu Shao, Dongsheng Zhang, Yuanqiang Mai, Yongwang Li, Flemming Besenbacher, Hans Niemantsverdriet, Federico Rosei, Jun Zhong, and Ren Su**

Abstract: Heterogeneous catalytic ammoxidation provides an eco-friendly route for the cyanide-free synthesis of nitrile compounds, which are important precursors for synthetic chemistry and pharmaceutical applications. However, in general such a process requires high pressures of molecular oxygen at elevated temperatures to accelerate the oxygen reduction and imine dehydrogenation steps, which is highly risky in practical applications. Here, we report an electric field enhanced ammoxidation system using a supported Fe clusters catalyst (Fe/NC), which enables efficient synthesis of nitriles from the corresponding aldehydes under ambient air pressure at room temperature (RT). A synergistic effect between the external electric field and the Fe/NC catalyst promotes the ammonia activation and the dehydrogenation of the generated imine intermediates and avoids the unwanted backwards reaction to aldehydes. This electric field enhanced ammoxidation system presents high efficiency and selectivity for the conversion of a series of aldehydes under mild conditions with high durability, rendering it an attractive process for the green synthesis of nitriles with fragile functional groups.

Introduction

Nitriles are important components in chemical syntheses that are widely employed in the agrochemical, dye, pharmaceutical, and polymer industry.[1] Aromatic nitriles are also used as key intermediates for the synthesis of amines, amides, oximes, tetrazoles and aldehydes.[2] Nitriles can be synthesized from halides with metal cyanides via Sandmeyer reaction[3] or Rosenmund-von Braun reactions (Scheme 1A),[4] though the needs of toxic precursors and the harsh reaction conditions mark it an environmentally unfriendly process.[1a,2a,5] Heterogeneous catalytic ammoxidation of hydrocarbons is the most employed process for the synthesis of nitriles in industry.[6] The so called Sohio process accounts for a dominant portion in the production of acrylonitrile and a series of nitriles production, by converting hydrocarbons into the corresponding nitriles with ammonia and pressurized oxygen at elevated temperatures, employing transition metal oxides as catalysts (Scheme 1B).[7] The reaction is highly exothermic, thus requiring strict heat control using cooling coils incorporated in the reactor. Another concern is the need of high-pressure oxygen (>1 bar), which poses a potential risk to operation, especially at high temperatures. Additionally, significant quantities of HCN and acetonitrile form as byproducts.[8]

A series of heterogeneous catalysts has been developed to improve the efficiency and selectivity of ammoxidation under close to ambient conditions.[9] Jagadeesh et al. show that supported metal oxides (Fe_2O_3 and Co_3O_4) catalyze at 130 °C (Scheme 1B).[10] Satisfactory catalytic performance is achieved owing to a rapid aerobic oxidation of alcohol to the corresponding aldehyde and an accelerated dehydrogenation of imine, promoted by a high loading of metal particles (≈6 mol %) and a high pressure of oxygen (5 bar). Recently, supported cluster and single-atom catalysts (SACs) have shown potential for economical and eco-friendly ammoxida-

---

[*] C. Wang, J. Li, T. Shao, D. Zhang, Y. Mai, Prof. Dr. R. Su
Soochow Institute for Energy and Materials InnovationS (SIEMIS), Soochow University
Suzhou, 215006 (China)
E-mail: suren@suda.edu.cn

C. Wang, J. Li, T. Shao, D. Zhang, Y. Mai, Prof. Dr. Y. Li, Prof. Dr. H. Niemantsverdriet, Prof. Dr. R. Su
SynCat@Beijing Synfuels China Technology Co. Ltd.
Leyuan South Street II, No.1, Yanqi Economic Development Zone C#, Beijing, 101407 (China)

Prof. Dr. Y. Li
State Key Laboratory of Coal Conversion, Institute of Coal Chemistry, CAS
Taiyuan, 030001 (China)

Prof. Dr. F. Besenbacher
Interdisciplinary Nanoscience Center, Aarhus University
Gustav Wieds Vej 14, 8000 Aarhus (Denmark)

Prof. Dr. H. Niemantsverdriet
Syngaschem BV
Valeriaanlaan 16, 5672 XD Nuenen (The Netherlands)

Prof. Dr. F. Rosei
Department of Chemical and Pharmaceutical Sciences, University of Trieste
Via Giorgeri 1, 34127 Trieste (Italy)

Prof. Dr. J. Zhong
Institute of Functional Nano and Soft Materials Laboratory (FUNSOM), Soochow University
Suzhou, 215123 (China)
E-mail: jzhong@suda.edu.cn

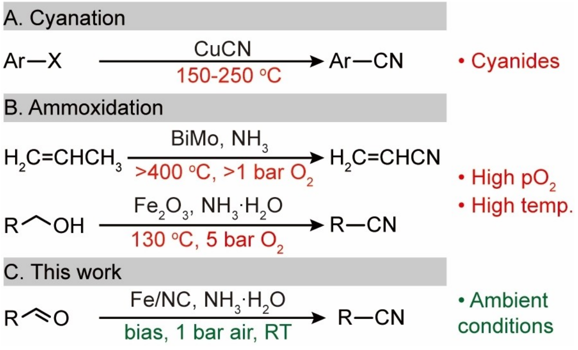

Scheme 1. Synthesis routes of nitriles via cyanation (A), ammoxidation (B), and electric field enhanced ammoxidation (C).

tion. Wang et al. has developed a Ru/MnO_2 catalyst for the ammoxidation of alcohols at 100–130 °C.[11] The highly dispersed Ru accelerates the dissociation of C–H bonds and activation of molecular oxygen with high tolerance for concentrated ammonia at a relatively low temperature; yet a high pressure of oxygen ($\approx$5 bar) is still required to achieve satisfactory conversion. Very recently, Fe and Co-based SACs have been found to exhibit remarkable efficiencies in activating both ammonia and oxygen, making them promising candidates for ammoxidation reactions.[12] Remarkably, Sun et al. report that the supported Fe SACs can promote the oxidation of benzyl alcohol in the presence of ammonia under atmospheric air at 35 °C, thus achieving an efficient ammoxidation under ambient conditions.[12a] Though high temperature ($\approx$140 °C) and pressure ($\approx$30 bar air) are still required to maintain catalyst stability as well as for the synthesis of some complicated nitriles, the strategy of employing clusters or SACs catalysts seems promising.

The ammoxidation under ambient conditions may be achieved by applying an external field to boost rate determining steps (RDS), such as the activation of ammonia, molecular oxygen, and certain intermediates. Such a strategy has been adopted in many important catalytic reactions by applying external magnetic or electric fields, or mechanical agitation,[13] which help to enhance charge transfer at phase boundaries between the catalysts and the reactants.[14] Wang et al. state that application of electric- and magnetic- fields has significant impact on the light absorption, charge carrier separation, and surface reactions in many photocatalytic reactions.[13b] Yao et al. reveal that the presence of external electric fields can regulate the adsorption affinity for hydrogen and water on various electrocatalysts, yielding enhanced performances for hydrogen and oxygen evolution reactions.[14b] Additionally, magnetic fields may also alternate electronic interactions between the catalyst and the adsorbed reactants to optimize the catalytic performance.[15] Therefore, we anticipate that the introduction of an external electric field along with cluster catalyst that exhibits ferromagnetic properties may modulate the interaction with hydrocarbons, oxygen, and ammonia, thus achieving improved ammoxidation performance under ambient conditions. Previous work in electrochemical cyanation and dehydrogenation of amines shows the possibility of nitrile synthesis under mild conditions,[1c,16] yet the ammoxidation using aqueous ammonia remains a challenging task.

Herein, we show that environmental ammoxidation of aldehydes can be realized by dispersing the Fe clusters supported on nitrogen doped carbon nanosheets (Fe/NC) in the reaction medium with an external electric field (Scheme 1C). A synergistic effect between the external electric field and the Fe/NC catalyst is observed according to reaction kinetics and the radical species investigations, which promotes the activation of ammonia and the dehydrogenation of the generated imine intermediate, thus avoiding unwanted backward reactions. Additionally, the system presents a high stability for the synthesis of a series of nitriles under ambient air pressure at RT, rendering it a promising ammoxidation process.

Results and Discussion

The Fe clusters supported on nitrogen doped carbon nanosheets (Fe/NC) is synthesized via a modified pyrolysis process according to previously reported methods (Notes S1 and S2).[17] A pyrrole-iron complex is used as the precursor with a sodium chloride as the template to yield highly wrinkled graphene-like Fe/NC nanosheets according to scanning electron microscopy imaging (SEM, Figure 1a). The as-synthesized Fe/NC possesses a large specific surface areas (858 $m^2 g^{-1}$, Figure S1), which is superior to that of SACs prepared from metal–organic frameworks (MOFs) based precursors,[12a,c] thus benefiting the adsorption and mass transfer of reactants for the ammoxidation process.

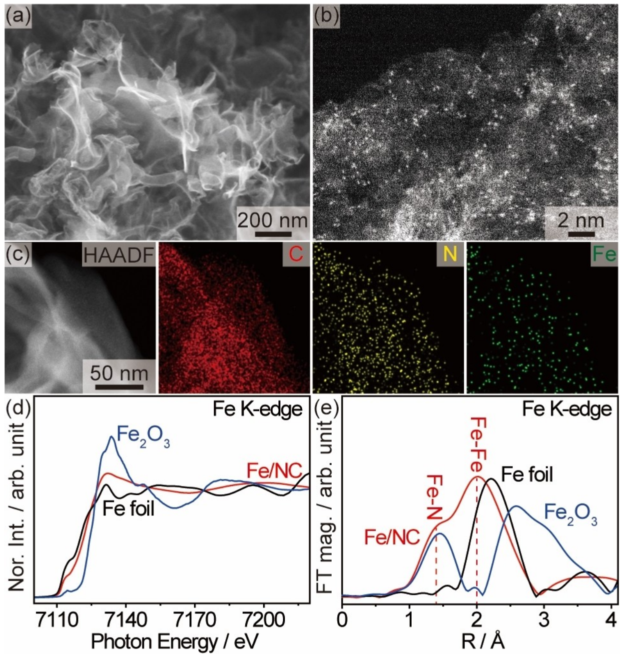

Figure 1. Characterization of the catalyst. a)–c) SEM, HAADF-STEM, and EDS mapping of the Fe/NC catalyst. d) and e) XANES and FT EXAFS spectra of the Fe/NC catalyst in comparison with a Fe foil and a Fe_2O_3 powder sample.

Aberration-corrected high-angle annular dark-field scanning transmission electron microscopy (HAADF-STEM) shows that tiny bright dots (<0.5 nm) are homogeneously distributed on the support, confirming the successful loading of highly dispersed Fe clusters (Figure 1b and S2). Energy-dispersive X-ray spectroscopic mapping proves that N, C, and Fe are uniformly distributed throughout the nanosheets (EDS, Figure 1c). Powder X-ray diffraction (XRD) of the NC support and the Fe/NC show similar diffraction patterns, with two broad peaks from the (002) and (101) planes of graphitic carbon (Figure S3). No metallic Fe diffraction peaks are detected due to the small size and low loading (≈ 0.5 wt %) according to inductively coupled plasma atomic emission spectrometry (ICP-AES, Table S1). These results are consistent with the Raman and X-ray photoelectron spectroscopy results (XPS, Figures S4 and S5), indicating that the Fe clusters do not agglomerate into larger metallic Fe nanoparticles (NPs) during the pyrolysis process.

The chemical state and coordination of the Fe species at the atomic level are studied by X-ray absorption near-edge structure (XANES) and extended X-ray absorption fine structure (EXAFS, Figures 1d and 1e). The K-edge of the Fe species in the Fe/NC is positioned closer to that of a standard Fe foil than that of Fe_2O_3 (Figure 1d). Additionally, the small peak at ≈ 7114 eV observed for the Fe/NC can be assigned to the fingerprint of Fe-N_4 square-planar structure, which originates from the 1 s→4pz transition and the associated charge transfer between the ligand and the metal.[12a,18] Fourier transform (FT) EXAFS spectra of Fe/NC reveal two distinct peaks at ≈ 1.44 Å and 2.0 Å, which can be indexed to the Fe–N and the Fe–Fe coordination of the supported Fe clusters, respectively (Figure 1e).[19] A shorter Fe–Fe bond length is observed for the Fe/NC compared with the Fe foil, which is possibly due to the compression by adjacent C and N atoms[20] and might be beneficial for O_2 adsorption and dissociation.[12c,19] The surface chemical compositions and oxidation states of Fe/NC have been also investigated by X-ray photoelectron spectroscopy (XPS, Figure S5). Only a very weak signal of the Fe2p peaks is observed for the Fe/NC, which does not warrant conclusions on the state of irons.

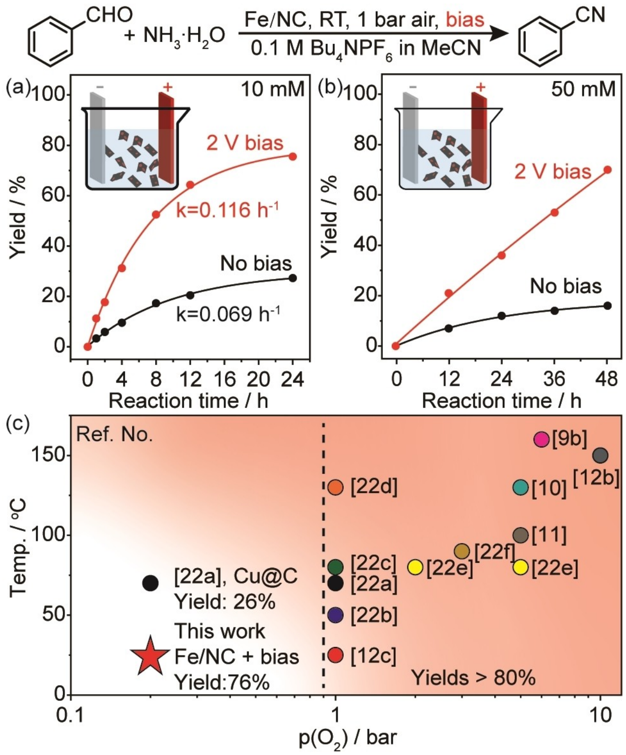

Figure 2. Ammoxidation of benzaldehyde using Fe/NC without and with external electric field. a) 10 mM and b) 50 mM benzaldehyde. Reaction conditions: benzaldehyde (0.1 or 0.5 mmol) and 1 mL $NH_3 \cdot H_2O$ (aq.) in 9 mL Bu_4NPF_6/MeCN solution (0.1 M) with 4 mg catalyst under continuous stirring for thermal catalysis. Additional carbon paper anode, Pt cathode, and a bias of 2 V are employed for electric field enhanced ammoxidation. All experiments were performed under atmospheric air and at RT. (c) Comparison of the electric field enhanced ammoxidation with reported thermal catalytic processes.

Benzaldehyde (**1a**, 10 mM) ammoxidation is employed as the model reaction to evaluate the effect of electric-field for the synthesis of benzonitrile in an aqueous ammonia-acetonitrile solution under RT and atmospheric conditions (Note S3). A modest yield of ≈ 20 % is observed in the absence of electric field, demonstrating an inefficient ammoxidation via the conventional thermal catalytic approach (Figure 2a). Interestingly, a significant improvement in yield is observed when a pair of electrodes (carbon paper as anode and Pt as cathode) are immersed into the suspension with the addition of Bu_4NPF_6 electrolyte (0.1 M) at a bias of 2 V (Figure 2a). A high selectivity to benzonitrile (90 %) is maintained for the whole course. Carbon and Pt are selected as anode and cathode to avoid unwanted electrocatalytic reactions, which reduce the conversion of benzaldehyde (Table S3). Note that an electric field alone in the absence of the Fe/NC or the presence of other metal cluster catalysts does not work (Table S2). The presence of electrolyte increases the dielectric permittivity of the medium, which benefits the polarization of the reactant molecules, thus resulting in enhanced catalytic performance (Figure S6).[21] However, the catalyst will be surrounded by electrolyte at higher concentrations (>0.1 M), causing a reduced contact of the reactants with catalyst and thus a poor performance. Remarkably, the electric field enhanced ammoxidation also operates at a higher starting concentration of **1a** (50 mM, Figure 2b). A comparable yield to that at low concentration is achieved for a reaction time of 48 h under a bias of 2 V, whereas the Fe/NC alone shows a much smaller yield of benzonitrile (<20 %). These results indicate a synergistic effect of the Fe/NC catalyst and the electric field in boosting the ammoxidation under ambient conditions. Additionally, only minor oxygen evolution (OER) and hydrogen evolution reactions (HER) are observed for the anodic and cathodic scans according to linear sweep voltammetry (LSV, Figure S7), implying that the electrochemical process exhibits a negligible contribution to the ammoxidation (Table S2). Figure 2c presents a literature survey of conditions applied in heterogeneous catalytic ammoxidation. High partial pressures of oxygen ($p(O_2)$) are generally required to achieve a satisfactory yields (>80 %).[9b,10–11,12b,c,22] Noticeably, a drastic decrease of yield is observed for the Cu supported on carbon catalyst (Cu@C) under ambient p(O_2) at elevated temperature (70 °C), highlighting the effect of electric field in boosting the ammoxidation under ambient conditions.

We have further explored the versatility of electric-field enhanced ammoxidation by Fe/NC for practical applications. A high conversion and selectivity is maintained within a wide range of benzaldehyde concentrations by simply adjusting the reaction time accordingly, suggesting control for production at larger scale is feasible (Figure 3a). In comparison, the concentration of ammonia dictates the conversion of benzaldehyde and selectivity to benzonitrile (Figure 3b). In the absence of ammonia, benzaldehyde partially converts into benzoic acid without the formation of benzonitrile, confirming that nitrogen originates solely from the activation of ammonia rather than from the catalyst or the solvent. An optimized concentration window of 1–3 M is preferred, and exposures to ammonia that are either too low or too high result in sharp drops in selectivity. The later is attributed to the formation of benzamide due to the hydrolysis of benzonitrile under alkaline conditions (Figure S8).[11] Additionally, the electric field enhanced ammoxidation can be performed by employing NH_4OAc as the N source (Entry 17, Table S2). Other inorganic nitrogen containing salts are inactive, possibly due to their poor solubility in MeCN (Table S2, Entries 18–20).

The applied bias is another crucial parameter that influences the conversion and selectivity of the ammoxidation process (Figure 3c). While increasing the bias from 0 to 2 V leads to a significant enhancement in conversion to nitrile at high selectivity, further increase of the bias results in the formation of benzil and benzamide, and thus a drop in selectivity to the nitrile. This is possibly caused by a rapid reduction of molecular oxygen and over oxidation of the reaction intermediates under high bias. It is also worth noting that a reasonable conversion (64 %) and excellent selectivity (92 %) is achieved under a bias of 1.5 V. This corresponds to an anodic bias of 1.5 V vs. reversible hydrogen electrode (RHE) and a cathodic bias of 0 V vs. RHE, respectively, under which conditions no HER and OER occur. For comparison, the electrochemical system shows poor conversion and selectivity under similar reaction conditions (entries 9 and 10, Table S2), conforming the vital role of external electric field. Interestingly, decent to high ammoxidation performances are also observed when employing Co/NC, Cu/NC, and FeCo/NC catalysts under electric field, featuring Fe/NC the optimum catalyst in terms of performance and cost (Figure S9). This shows the generality of the electric field effect in the ammoxidation reaction. The effect of pulsed bias has been also evaluated (Figure S10). While the selectivity remains high at all conditions, a slight drop of the conversion is observed. This again implies that the process is an electric field enhanced process rather than an electrochemical process, The alternated electric field may change the polarization of the molecule, causing unwanted reverse reaction of the generated intermediates and resulting in a decrease of the conversion.

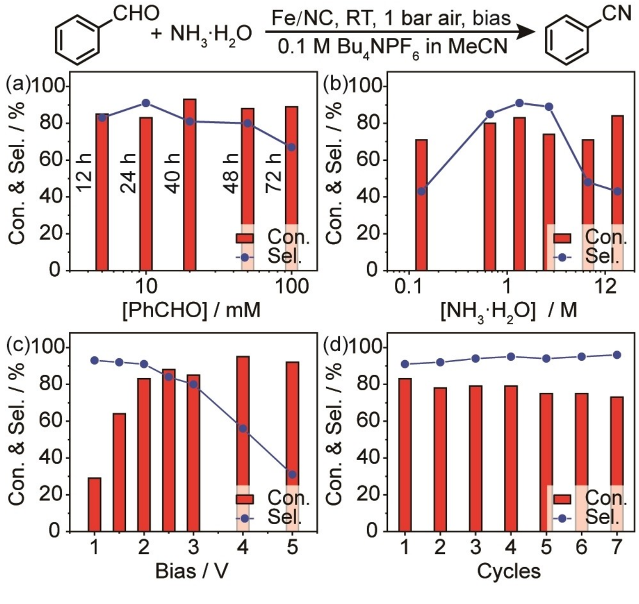

Figure 3. Electric field enhanced ammoxidation of benzaldehyde. a)–c) Effects of starting concentration of benzaldehyde, $NH_3 \cdot H_2O$ concentration and bias. d) Reusability of Fe/NC. Reaction conditions: desired amount of benzaldehyde and $NH_3 \cdot H_2O$ (aq.) in Bu_4NPF_6/MeCN solution (0.1 M) with 4 mg catalyst under continuous stirring, carbon paper anode, Pt cathode, and a desired bias. All experiments were performed under atmospheric air pressure and RT. The concentration of benzaldehyde is 10 mM for b)–d).

The Fe/NC catalyst shows a durable performance for seven consecutive cycles without noticeable reduction in activity and selectivity under a bias of 2 V, demonstrating a high stability of the catalyst for ammoxidation under ambient conditions (Figure 3d). *Post mortem* characterizations of the spent catalyst by SEM, XPS and ICP-AES confirm that there is no obvious change of the Fe/NC after long term operation (Table S1, Figure S11 and S12).

The promotional mechanism of the electric field on the ammoxidation reaction has been investigated by following the reaction intermediates and radical species (Figure 4). According to previous investigations, aldehyde and ammonia can undergo a nucleophilic substitution reaction, resulting in the formation of unstable hemiaminal that eventually converts into imine under ambient conditions via dehydration in the absence of a catalyst.[9a,22f,23] The generated imine can either turn back into aldehyde reversibly or converts into nitrile via dehydrogenation in the presence of a proper catalyst, and thus it is the key intermediate and step to achieve efficient ammoxidation.

To evaluate the effect of electric field and catalyst in ammoxidation, we have first obtained a relatively high concentration of the hemiaminal and benzimine intermediate in a Bu_4NPF_6/MeCN solution (Figure S13). This is realized by adding benzaldehyde into concentrated aqueous ammonia, yielding white sediments that are rich of hemiaminal and benzimine intermediates and is eventually added into the Bu_4NPF_6/MeCN solution (Note S4 and Figure S13–S14). While imine is gradually consumed at a similar rate regardless of the presence of catalyst or bias (Figure 4a), a

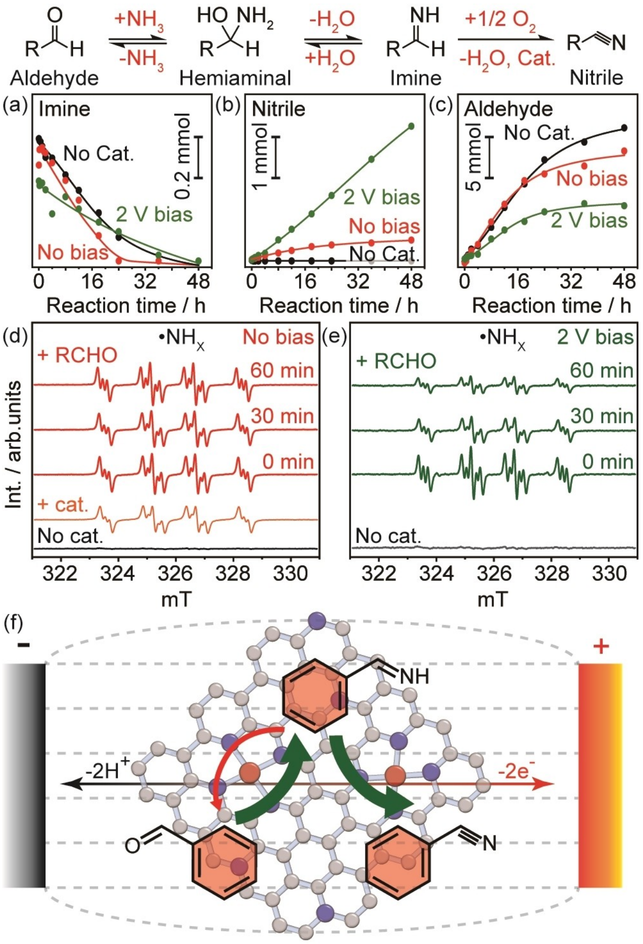

Figure 4. Mechanistic analysis. a)–c) Evolutions of imines, nitrile, and aldehyde starting from generated imines. Reaction conditions: freshly synthesized imines added in Bu_4NPF_6/MeCN (0.1 M) under continuous stirring. Detailed reaction conditions are provided in Note S4. d) and e) Evolution of radical species without and with bias using DMPO as the spin trap. Reaction conditions: 4 mg Fe/NC, 50 mM benzaldehyde, and 20 mM DMPO in a 400 μL $NH_3\cdot H_2O$-MeCN solution (6.7 M $NH_3\cdot H_2O$). f) Promotional mechanism of electric field enhanced ammoxidation with supported Fe cluster catalyst.

significant accumulation of nitrile is only observed in the presence of the Fe/NC under bias (Figure 4b). Considering the absence of nitrile without a catalyst, it indicates that the dehydrogenation of imine is not a spontaneous step and can be promoted by applying a bias. Remarkably, the external bias also slows down the reversible conversion of imine back to aldehyde (Figure 4c), thus resulting in an enhanced efficiency for ammoxidation reactions. We have also analyzed the evolution of reactants, intermediates, and products in the presence of ammonia (Figure S15). Again, the external electric field accelerates the evolution of nitrile while it inhibits the formation of aldehyde in the presence of ammonia. Note the addition of ammonia also introduces water into the system, thus promoting the hydrolysis of imine while preventing the formation of aldehyde. Additionally, the presence of electrolyte may also promote the ionization of generated water molecules, thus driving protons and hydroxides into anode and cathodes for HER and OER, shifting the reaction equilibrium towards the formation of nitriles (Figure S16).

The effect of an external electric field is further investigated by electron paramagnetic resonance (EPR) using DMPO as the spin trap (Note S5). While no radical species are observed in the absence of Fe/NC in a $NH_3\cdot H_2O$-MeCN solution (6.7 M $NH_3\cdot H_2O$), the $^{\bullet}NH_x$ radicals appear when Fe/NC is added into the solution (Figure 4d),[24] suggesting that the Fe/NC can activate $NH_3\cdot H_2O$ molecules under ambient conditions. Noticeably, the addition of benzaldehyde does not significantly influence the intensity of the $^{\bullet}NH_x$ signal even at prolonged reaction times (Figure 4d, red curves). Since the $^{\bullet}NH_x$ radical can also react with benzaldehyde to generate hemiaminal and eventually into imine, a constant intensity of the $^{\bullet}NH_x$ radical indicates that an equilibrium between benzaldehyde and the hemiaminal is reached when the Fe/NC catalyst is present. In comparison, a gradual decrease of the $^{\bullet}NH_x$ signal is observed upon increasing the reaction time in the presence of an external electric field (Figure 4e, green curves), implying that a shift of the reaction equilibrium in forward direction, thus suppressing the reversible conversion of imine back to benzaldehyde.

The synergistic effect between the Fe/NC catalyst and the external electric field in promoting the ammoxidation of aldehyde is schematically presented in Figure 4f. Prior to the formation of nitriles, the imine intermediates are generated spontaneously when aldehyde reacts with aqueous ammonia. While the Fe/NC slightly improves the dehydrogenation rate of imines, the rate of the reverse reaction of imine remains unchanged, resulting in a slight shift of the reaction equilibrium towards the formation of nitriles. The addition of an external electric field not only strongly boosts the dehydrogenation rate of imines, but also suppresses the backward hydrolysis of imines to aldehydes markedly, leading to the optimized ammoxidation of aldehydes under ambient conditions.

The Fe/NC catalyst with external electric field exhibits satisfactory ammoxidation performances for the synthesis of complicated nitriles under ambient conditions with decent carbon balances (Table 1, Table S4, and Figures S17–S37). All aromatic aldehydes (**3a**–**3o**) show considerably high conversion to target nitriles with excellent selectivity. The presence of electron withdrawing groups (EWG, **3b**–**3f**) and electron donating groups (EDG, **3g**–**3l**) on the aromatic aldehydes does not significantly affect the conversion efficiency for the synthesis of the corresponding nitriles under 1 bar air at RT. Noticeably, the halogen functional groups on the aromatic aldehydes can be well preserved for selective synthesis of halogenated benzonitriles (**3b**–**3d**), which are important building blocks for the pharmaceutical and the dye industry.[11] The ammoxidation of cycloalkanes also shows excellent conversion and selectivity to the corresponding nitriles (>90 %, **3p** and **3q**), indicating a negligible effect of the electrophilicity of the carbonyls, possibly due to the addition of the electric field. A reduced selectivity is observed for the synthesis of cyanocyclohexene (**3r**) from formylcyclohexene, possibly due to the compet-

Table 1: Substrates scope. Electric-field enhanced ammoxidation of aldehydes using Fe/NC under ambient $p(O_2)$ and RT.

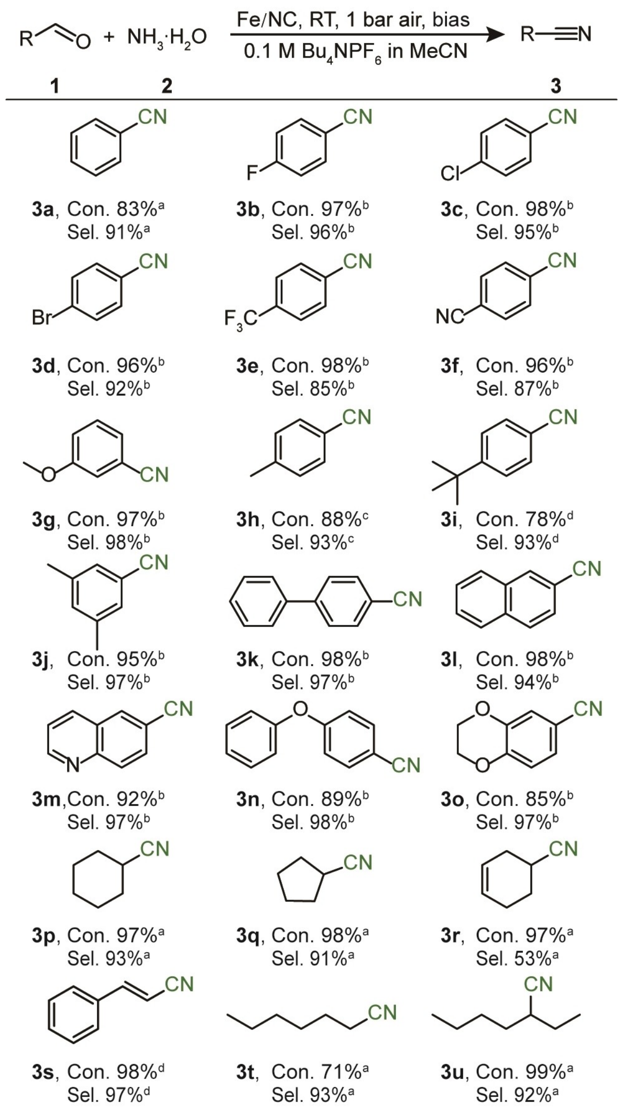

$$\mathbf{1}\ R\text{-CHO} + \mathbf{2}\ NH_3\cdot H_2O \xrightarrow[\text{0.1 M } Bu_4NPF_6 \text{ in MeCN}]{\text{Fe/NC, RT, 1 bar air, bias}} \mathbf{3}\ R\text{-C}\equiv N$$

Product	Con.	Sel.
3a	83%^{a}	91%^{a}
3b	97%^{b}	96%^{b}
3c	98%^{b}	95%^{b}
3d	96%^{b}	92%^{b}
3e	98%^{b}	85%^{b}
3f	96%^{b}	87%^{b}
3g	97%^{b}	98%^{b}
3h	88%^{c}	93%^{c}
3i	78%^{d}	93%^{d}
3j	95%^{b}	97%^{b}
3k	98%^{b}	97%^{b}
3l	98%^{b}	94%^{b}
3m	92%^{b}	97%^{b}
3n	89%^{b}	98%^{b}
3o	85%^{b}	97%^{b}
3p	97%^{a}	93%^{a}
3q	98%^{a}	91%^{a}
3r	97%^{a}	53%^{a}
3s	98%^{d}	97%^{d}
3t	71%^{a}	93%^{a}
3u	99%^{a}	92%^{a}

Reaction conditions: [a]0.1 mmol substrates, 4 mg Fe/NC, carbon paper as anode, Pt as cathode, 1 mL aq. $NH_3\cdot H_2O$ (aq.), 9 mL Bu_4NPF_6/MeCN (0.1 M), 2 V, 24 h. [b]2 mL $NH_3\cdot H_2O$ (aq.), 8 mL Bu_4NPF_6/MeCN (0.1 M), 2.5 V, 36 h. [c]2 mL $NH_3\cdot H_2O$ (aq.), 8 mL Bu_4NPF_6/MeCN (0.1 M), 2 V, 48 h. [d]2 mL $NH_3\cdot H_2O$ (aq.), 8 mL Bu_4NPF_6/MeCN (0.1 M), 2 V, 36 h. The products were determined by GC-MS analysis. Conversion (Con.) and selectivity (Sel.) were determined by GC.

itive polymerization of the precursor. Remarkably, aliphatic nitriles (**3s**–**3u**) can also be synthesized with high selectivity and conversion from their corresponding aldehydes under ambient oxygen pressure at RT by the electric-field enhanced ammoxidation system. Note that the synthesis of these nitriles via ammoxidation normally requires high $p(O_2)$ at high temperature to achieve reasonable performance.[11–,12c] Additionally, isolated yields of 60–70 % can be achieved for gram-scale synthesis of **3k** and **3s**, which are important chemicals for pigment and spice industries (Fig S38). Moreover, perillyl aldehyde, myrtenal and citral, which are important biomass-derived aldehydes, can be selectively converted into corresponding nitriles (Figures S39–S42), offering an economic route for spice chemistry.

Conclusion

In summary, we present a sustainable system for catalytic ammoxidation of aldehydes under ambient oxygen pressure and at room temperature by employing supported Fe cluster catalyst in an external electric field. The synergy between the Fe/NC catalyst and the electric-field enables efficient synthesis of nitriles due to the enhanced activation of ammonia and accelerated dehydrogenation of the generated imine intermediates, which avoids unwanted reversible reactions. The electric field enhanced ammoxidation approach shows excellent durability, activity and selectivity for the synthesis of nitriles containing various functional groups, thus rendering it an attractive process for the eco-friendly synthesis of nitriles. The mild conditions of the electric field enhanced ammoxidation reduce the cost of construction and operation for scaling up, and also positively impact the crafting of biomass-derived aldehydes with fragile functional groups that are vulnerable under conventional ammoxidation conditions.

Acknowledgements

RS thanks the NSFC (project No.: 21972100). JZ acknowledges the National Key R&D Program of China (2020YFA0406103). We also thank the Project of Innovation and Entrepreneurship of Jiangsu Province (grant No.: JSSCRC202010539) and the Suzhou Foreign Academician Workstation (project No.: SWY2022001) for financial supports. We also acknowledge support from the Soochow Municipal Laboratory for Low Carbon Technologies and Industries.

Conflict of Interest

The authors declare no conflict of interest.

Data Availability Statement

The data that support the findings of this study are available in the supplementary material of this article.

Keywords: Ammoxidation · Electric Field · Heterogeneous Catalysis · Nitriles · Supported Clusters

---

[1] a) J. Kim, H. J. Kim, S. Chang, *Angew. Chem. Int. Ed.* **2012**, *51*, 11948–11959; b) G. Yan, Y. Zhang, J. Wang, *Adv. Synth. Catal.* **2017**, *359*, 4068–4105; c) H. Hu, S. Wu, F. Yan, M. Makha, Y. Sun, C.-X. Du, Y. Li, *J. Energy Chem.* **2022**, *70*, 542–575.

[2] a) P. Anbarasan, T. Schareina, M. Beller, *Chem. Soc. Rev.* **2011**, *40*, 5049–5067; b) R. D. Patil, M. K. Gupta, *Adv. Synth. Catal.* **2020**, *362*, 3987–4009.

[3] a) I. P. Beletskaya, A. S. Sigeev, A. S. Peregudov, P. V. Petrovskii, *J. Organomet. Chem.* **2004**, *689*, 3810–3812; b) F. Mo, G. Dong, Y. Zhang, J. Wang, *Org. Biomol. Chem.* **2013**, *11*, 1582.

[4] a) Q. Zhang, D. Ma, *Synlett* **2023**, *34*, 1395–1398; b) J. X. Wu, B. Beck, R. X. Ren, *Tetrahedron Lett.* **2002**, *43*, 387–389.

[5] a) T. Schareina, A. Zapf, M. Beller, *Chem. Commun.* **2004**, 1388–1389; b) J. Zanon, A. Klapars, S. L. Buchwald, *J. Am. Chem. Soc.* **2003**, *125*, 2890–2891; c) C. Yang, J. M. Williams, *Org. Lett.* **2004**, *6*, 2837–2840; d) P. Pollak, G. Romeder, F. Hagedorn, H.-P. Gelbke, *Ullman's Encyclopedia of Industrial Chemistry*, Wiley-VCH, Weinheim, **2000**, pp. 251–263.

[6] a) B. Chen, L. Zhang, H. Luo, L. Huang, P. He, G. Xue, H. Liang, W. Dai, *JACS Au* **2023**, *3*, 476–487; b) E. M. Karp, T. R. Eaton, V. S. Nogué, V. Vorotnikov, M. J. Biddy, E. C. D. Tan, D. G. Brandner, R. M. Cywar, R. Liu, L. P. Manker, W. E. Michener, M. Gilhespy, Z. Skoufa, M. J. Watson, O. S. Fruchey, D. R. Vardon, R. T. Gill, A. D. Bratis, G. T. Beckham, *Science* **2017**, *358*, 1307–1310; c) S. G. Davey, *Nat. Chem. Rev.* **2018**, *2*, 0110.

[7] T. A. Hanna, *Coord. Chem. Rev.* **2004**, *248*, 429–440.

[8] a) D. P. Hansora, *Industrial manufacturing process of Acrylonitrile*, LAP LAMBERT Academic Publishing, London, **2014**, pp. 41–53; b) F. Rezaie, V. Pirouzfar, A. Alihosseini, *Therm. Sci. Eng. Prog.* **2020**, *16*, 100463.

[9] a) T. Senthamarai, V. G. Chandrashekhar, N. Rockstroh, J. Rabeah, S. Bartling, R. V. Jagadeesh, M. Beller, *Chem* **2022**, *8*, 508–531; b) X. Liu, J. Qin, W. Dai, Z. Zhu, P. Zhou, Y. Wang, J. Nie, Y. Yang, Z. Zhang, *ACS Catal.* **2022**, *12*, 13300–13311; c) T. Yasukawa, X. Yang, S. Kobayashi, *J. Org. Chem.* **2020**, *85*, 7543–7548.

[10] R. V. Jagadeesh, H. Junge, M. Beller, *Nat. Commun.* **2014**, *5*, 4123.

[11] H. Wang, D. Xu, E. Guan, L. Wang, J. Zhang, C. Wang, S. Wang, H. Xu, X. Meng, B. Yang, B. C. Gates, F.-S. Xiao, *ACS Catal.* **2020**, *10*, 6299–6308.

[12] a) K. Sun, H. Shan, H. Neumann, G. P. Lu, M. Beller, *Nat. Commun.* **2022**, *13*, 1848; b) H. Luo, S. Tian, H. Liang, H. Wang, S. Gao, W. Dai, *Nat. Commun.* **2023**, *14*, 2981; c) J. Qin, B. Han, X. Liu, W. Dai, Y. Wang, H. Luo, X. Lu, J. Nie, C. Xian, Z. Zhang, *Sci. Adv.* **2022**, *8*, eadd1267.

[13] a) X. Li, W. Wang, F. Dong, Z. Zhang, L. Han, X. Luo, J. Huang, Z. Feng, Z. Chen, G. Jia, T. Zhang, *ACS Catal.* **2021**, *11*, 4739–4769; b) Z. Wang, Y. Li, C. Wu, S. C. E. Tsang, *Joule* **2022**, *6*, 1798–1825; c) Y. Xu, Z. Zhou, M. Zou, Y. Liu, Y. Zheng, Y. Yang, S. Lan, J. Lan, C.-W. Nan, Y.-H. Lin, *Mater. Today* **2022**, *54*, 225–246; d) J. Zhao, X. Zhang, J. Xu, W. Tang, Z. Lin Wang, F. Ru Fan, *Angew. Chem. Int. Ed.* **2023**, *62*, e202300604.

[14] a) G. Pacchioni, J. R. Lomas, F. Illas, *J. Mol. Catal. A* **1997**, *119*, 263–273; b) J. Yao, W. Huang, W. Fang, M. Kuang, N. Jia, H. Ren, D. Liu, C. Lv, C. Liu, J. Xu, Q. Yan, *Small Methods* **2020**, *4*, 2000494.

[15] C. Biz, M. Fianchini, J. Gracia, *ACS Catal.* **2021**, *11*, 14249–14261.

[16] a) H. Yang, Y. Shen, Z. Xiao, C. Liu, K. Yuan, Y. Ding, *Chem. Commun.* **2020**, *56*, 2435–2438; b) Q. Chen, C. Fang, Z. Shen, M. Li, *Electrochem. Commun.* **2016**, *64*, 51–55; c) X. Yang, Z. Fan, Z. Shen, M. Li, *Electrochim. Acta* **2017**, *226*, 53–59; d) M. T. Bender, K.-S. Choi, *JACS Au* **2022**, *2*, 1169–1180.

[17] M. Wang, S. Liu, T. Qian, J. Liu, J. Zhou, H. Ji, J. Xiong, J. Zhong, C. Yan, *Nat. Commun.* **2019**, *10*, 341.

[18] W. Liu, L. Zhang, X. Liu, X. Liu, X. Yang, S. Miao, W. Wang, A. Wang, T. Zhang, *J. Am. Chem. Soc.* **2017**, *139*, 10790–10798.

[19] W. Zhai, S. Huang, C. Lu, X. Tang, L. Li, B. Huang, T. Hu, K. Yuan, X. Zhuang, Y. Chen, *Small* **2022**, *18*, e2107225.

[20] Z. Ma, S. Liu, N. Tang, T. Song, K. Motokura, Z. Shen, Y. Yang, *ACS Catal.* **2022**, *12*, 5595–5604.

[21] R. J. LeSuer, C. Buttolph, W. E. Geiger, *Anal. Chem.* **2004**, *76*, 6395–6401.

[22] a) Y. Yoon, B. R. Kim, C. Y. Lee, J. Kim, *Asian J. Org. Chem.* **2016**, *5*, 746–749; b) K.-K. Sun, J.-L. Sun, G.-P. Lu, C. Cai, *Green Chem.* **2019**, *21*, 4334–4340; c) A. N. Hashemi, H. Eshghi, K. Lamei, *Appl. Organomet. Chem.* **2019**, *33*, e4835; d) S. Shang, L. Wang, W. Dai, B. Chen, Y. Lv, S. Gao, *Catal. Sci. Technol.* **2016**, *6*, 5746–5753; e) M. Hua, J. Song, X. Huang, H. Liu, H. Fan, W. Wang, Z. He, Z. Liu, B. Han, *Angew. Chem. Int. Ed.* **2021**, *60*, 21479–21485; f) Y. Preger, T. W. Root, S. S. Stahl, *ACS Omega* **2018**, *3*, 6091–6096.

[23] a) J.-F. Soulé, H. Miyamura, S. Kobayashi, *J. Am. Chem. Soc.* **2011**, *133*, 18550–18553; b) W. Wang, L. Ma, X. Jiang, H. Wang, Z.-H. He, K. Wang, Y. Yang, Z.-T. Liu, *ACS Sustainable Chem. Eng.* **2022**, *10*, 14636–14647.

[24] a) C. Chen, R. P. Veregin, J. R. Harbour, M. L. Hair, S. L. Issler, J. Tromp, *J. Phys. Chem.* **1989**, *93*, 2607–2609; b) C. F. Chignell, B. Kalyanaraman, R. H. Sik, R. P. Mason, *Photochem. Photobiol.* **1981**, *34*, 147–156.